

Dispersive representation and shape of the K_{l3} form factors: robustness.

Véronique Bernard ^{a,1}, Micaela Oertel ^{b,2}, Emilie Passemar ^{c,3} and Jan Stern ^{a, 4}

^a *Groupe de Physique Théorique, IPN, CNRS/Univ. Paris-Sud 11, 91406 Orsay Cedex, France*

^b *LUTH, Observatoire de Paris, CNRS, Univ. Paris Diderot, 5 place Jules Janssen, 92195 Meudon, France*

^c *Institute for theoretical physics, University of Bern, Sidlerstr. 5, 3012 Bern, Switzerland*

Abstract: An accurate low-energy dispersive parametrization of the scalar $K\pi$ form factor was constructed some time ago in terms of a single parameter guided by the Callan-Treiman low-energy theorem. A similar twice subtracted dispersive parametrization for the vector $K\pi$ form factor will be investigated here. The robustness of the parametrization of these two form factors will be studied in great detail. In particular the cut-off dependence, the isospin breaking effects and the possible, though not highly probable, presence of zeros in the form factors will be discussed. Interesting constraints in the latter case will be obtained from the soft-kaon analog of the Callan-Treiman theorem and a comparison with the recent $\tau \rightarrow K\pi\nu_\tau$ data.

arXiv:0903.1654v1 [hep-ph] 10 Mar 2009

¹Email: bernard@ipno.in2p3.fr

²Email: micaela.oertel@obspm.fr

³Email: passemar@itp.unibe.ch

⁴Jan Stern sadly passed away before the final version of the paper was written.

1 Introduction

Experimental information on the shape of the strangeness changing scalar $f_0(t)$ and vector $f_+(t)$ form factors in the low-energy region can be obtained from the study of $K_{\ell 3}$ -decays. $f_0(t)$ and $f_+(t)$ indeed enter the differential decay rates of these semi-leptonic processes. In the expression of these decay rates $f_0(t)$ is multiplied by a kinematic factor $(m_\ell/m_K)^2$ with m_ℓ and m_K the lepton and the kaon mass, respectively. This factor being of the order 10^{-6} for the electron, only the muon mode is, in fact, sensitive to the scalar form factor which is thus harder to determine. Different collaborations, namely ISTRA [1], KLOE [2, 3], KTeV [4, 5] and NA48 [6, 7] have measured these kaon decays. In the analysis of their data, they parametrize the two form factors in terms of some free parameters. The actual number of parameters which can be determined from a fit to the data are, due to strong correlations between them, at most two for the vector form factor and one for the scalar one. Thus quadratic-, pole- and more recently parametrizations based on conformal mapping (denoted z-parametrization) have been used for $f_+(t)$ while, up to recently $f_0(t)$ was described in terms of a linear and a pole one⁵. While the pole parametrization gives comparable results for $f_+(t)$ in the different experiments, the situation for f_0 was much more confused. The slope of the normalized scalar form factor, $\bar{f}_0(t)$, varied typically between $9 \cdot 10^{-3}$ and $15 \cdot 10^{-3}$ depending on the experiments [8]. Note that the slope determined in this way can only be an upper limit of the true mathematical slope $d\bar{f}_0(t)/dt|_{t=0}$ as calculated for example within chiral perturbation theory [9, 10]. Therefore it seemed appropriate, in particular in the case of the scalar form factor, to develop another parametrization which is as model independent as possible, involves only one parameter and determines the higher order terms in the series' expansion on physical ground. An accurate dispersive representation has been constructed in Ref. [11] which fulfills all these properties. Two classes of parametrizations can hence be distinguished depending on whether or not physical information is used. In the first class one finds for example the pole one for the vector form factor and this dispersive parametrization for the scalar form factor and in the second one the linear and the quadratic parametrizations. Strictly speaking the z-parametrization enters also this latter class. However, in Ref. [12] it was shown that under certain conditions it is possible to impose a bound on the sum of the expansion coefficients based on unitarity and the total rate of $\tau \rightarrow K\pi\nu_\tau$.

While the main aim of these $K_{\ell 3}$ experiments was to extract the CKM matrix element V_{us} the dispersive parametrization of \bar{f}_0 provides another test of the Standard Model (SM) through the measurement of the only unknown parameter $\ln C$, with C the value of the scalar form factor at the Callan Treiman (CT) point. This was in fact the original idea behind writing such a dispersive parametrization. It has first been used by the NA48 collaboration leading to a rather small slope for \bar{f}_0 and a 4.5σ deviation to the SM [7]. Unfortunately the situation is still unclear for the scalar form factor, recent determinations of $\ln C$ from KLOE [3] and KTeV [13] lead to no/slight discrepancy with the SM. Due to the importance of such a measurement it is very important to discuss in more detail the robustness of this dispersive parametrization. This is the main aim of this paper together with the investigation of a similar parametrization for the vector form factor improving on the pole parametrization.

⁵Note that in the case of the scalar form factor the lightest resonance, the κ^* , is rather broad. In addition, there is a second resonance not far away. Thus contrary to the vector form factor case, the parametrization of the scalar form factor in terms of one real pole has no physical motivation.

After introducing basic notations and properties in section 2 we will briefly review in section 3 the dispersive parametrization for the scalar form factor. We will then describe an analogous parametrization for the vector form factor. In section 4 we will investigate the robustness of these parametrizations for both, the scalar and the vector form factors. We will discuss the uncertainties due to the input parameters as well as the expected size of isospin breaking effects. In the dispersive parametrization the standard, since most likely, hypothesis of the absence of zeros in the form factor has been made. In section 4.3 we will question this hypothesis and in particular, we will study the presence of possible real or complex zeros in the form factors and the impact of these zeros on the value of $\ln C$. Even if the likelihood of such a scenario is small its study is required by the particular importance of an unambiguous test of the SM. The possibility of discarding zeros in the form factors from some properties of the scalar form factor as well as from a comparison with high energy data from τ -decays will be discussed in detail. We will conclude in section 5 and finally present some useful expressions to simplify the use of the dispersive parametrization in the data analysis in the appendix.

2 Basic definitions and properties

The hadronic matrix element describing $K_{\ell 3}$ -decays is written in terms of two form factors $f_+^{K\pi}(t)$ and $f_-^{K\pi}(t)$,

$$\langle \pi(p_\pi) | \bar{s} \gamma_\mu u | K(p_K) \rangle = (p_\pi + p_K)_\mu f_+^{K\pi}(t) + (p_K - p_\pi)_\mu f_-^{K\pi}(t), \quad (2.1)$$

where $t = (p_K - p_\pi)^2$. The vector form factor $f_+^{K\pi}(t)$ represents the P-wave projection of the crossed channel matrix element $\langle 0 | \bar{s} \gamma_\mu u | K\pi \rangle$, whereas the S-wave projection is described by the scalar form factor defined as

$$f_0(t) = f_+^{K\pi}(t) + \frac{t}{m_K^2 - m_\pi^2} f_-^{K\pi}(t). \quad (2.2)$$

In the following discussion we will consider the normalized form factors

$$\bar{f}_0(t) = \frac{f_0(t)}{f_+(0)} \quad \text{and} \quad \bar{f}_+(t) = \frac{f_+(t)}{f_+(0)} \quad \text{with} \quad \bar{f}_0(0) = \bar{f}_+(0) = 1, \quad (2.3)$$

and try to describe their shape as precisely as possible in the physical region of $K_{\ell 3}$ -decays, $m_\ell^2 \leq t \leq t_0 = (m_K - m_\pi)^2$, with m_π the pion mass. It is shown in Fig. 1 together with the right hand cut from $K\pi$ scattering which starts at $t_{K\pi} = (m_K + m_\pi)^2$ as well as the CT point $\Delta_{K\pi} = m_K^2 - m_\pi^2$ whose value is about twice as large as t_0 . This point is of special interest in the case of the scalar form factor. Indeed, the Callan-Treiman low-energy theorem [14] predicts its value in the $SU(2)$ chiral limit (where the quark masses $m_{u,d}$ vanish) at that particular point. As we will see, this is of great importance in testing the SM. For physical quark masses, one has

$$C \equiv \bar{f}_0(\Delta_{K\pi}) = \frac{F_{K^+}}{F_{\pi^+}} \frac{1}{f_+^{K^0\pi}(0)} + \Delta_{CT}, \quad (2.4)$$

where F_{K^+,π^+} are the charged kaon and pion decay constants, respectively, and Δ_{CT} is a correction of $\mathcal{O}(m_{u,d}/4\pi F_\pi)$ ⁶. It has been estimated within Chiral Perturbation Theory (ChPT) at

⁶Note that for practical purposes we have introduced some isospin breaking effects already in the first term on the right-hand side (RHS) of Eq. (2.4).

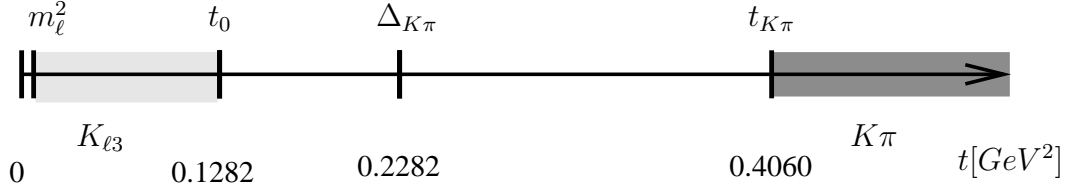


Figure 1: *Different energy scales involved in the analysis of the scalar and vector form factors: the physical region of $K_{\ell 3}$ -decays lies between the lepton mass squared m_ℓ^2 and $t_0 = (m_K - m_\pi)^2$, $\Delta_{K\pi} = m_K^2 - m_\pi^2$ denotes the CT point and the right-hand cut from $K\pi$ scattering starts at $t_{K\pi} = (m_K + m_\pi)^2$. For the numerical values, m_{K^+} and m_{π^0} have been used.*

next to leading order (NLO) in the isospin limit [15] with the result

$$\Delta_{CT}^{NLO} = (-3.5 \pm 8) \times 10^{-3}. \quad (2.5)$$

The error is a conservative estimate assuming typical size corrections of $\mathcal{O}(m_{u,d})$ and $\mathcal{O}(m_s)$ [16] for the higher orders. It should certainly hold for the neutral kaon decays which we are mainly interested in at present. Indeed, no large corrections to this estimate are expected due to the absence of π^0 - η mixing in the final state which could lead to small energy denominators. Eq. (2.5) is consistent with the values obtained recently, see Refs [10], [17] and [18]. The quantities entering the expression of C , Eq. (2.4), are in principle completely determined within QCD. Except for Δ_{CT} , they are studied within lattice QCD, see Ref. [19] for a recent overview of the situation. However, the actual most precise determinations of these quantities are obtained from semi-leptonic decays. Consequently, they depend on the assumption made for the electroweak couplings of quarks. Assuming the SM couplings, one can extract the quantity

$$B_{exp} = \left| \frac{F_{K^+} V_{us}}{F_{\pi^+} V_{ud}} \right| \frac{1}{|f_+^{K^0 \pi^+}(0) V_{us}|} |V_{ud}|, \quad (2.6)$$

using experimental information on the ratio $\Gamma_{K_{\ell 2}^+(\gamma)} / \Gamma_{\pi_{\ell 2}^+(\gamma)}$, the decay $K^0 \rightarrow \pi^- e \nu_e$ [20] and $0^+ \rightarrow 0^+$ transitions in nuclei [22]. These determine respectively the first ratio, the second one and $|V_{ud}|$ in Eq. (2.6) with high precision and lead to

$$B_{exp} = 1.2418 \pm 0.0039. \quad (2.7)$$

Interestingly the knowledge of V_{us} is unnecessary for determining B_{exp} . Eq. (2.4) then becomes

$$\begin{aligned} \ln C|_{SM} &= \ln B_{exp} + \Delta_{CT}/B_{exp} \\ &= 0.2166 \pm 0.0034 + (-0.0035 \pm 0.0080)/(1.2418 \pm 0.0039) \\ &= 0.2138 \pm 0.0073, \end{aligned} \quad (2.8)$$

where in the last line all the errors have been added in quadrature. Note that the error on $\ln C|_{SM}$ is rather small. Hence a precise measurement of $\ln C$ in neutral $K_{\mu 3}$ -decays should allow to test the SM electroweak couplings by comparing the obtained value with the one from Eq. (2.8). However, the Callan-Treiman point is unreachable by a direct measurement of this decay, its value being much larger than the end point value of the physical region, see figure 1. For this reason a dispersive representation of the scalar form factor written in terms of $\ln C$ as the only free parameter has been introduced in Ref. [11].

3 Dispersive parametrization

Let us first briefly review this dispersive parametrization of the scalar form factor based on an Omnès representation [23], see also Ref. [24] for an early application. We will then introduce a similar representation to accurately describe the vector form factor in the low energy region.

3.1 Scalar form factor

The dispersive representation of the scalar form factor introduced in Ref. [11] follows previous attempts to determine the form factor in the physical region. In Ref. [25] a coupled channel approach was used with only one subtraction in the dispersion relation. The main aim of Ref. [11] was to stay as model independent as possible. Therefore a second subtraction has been made in order to minimize the bad knowledge of the high energy region in the dispersive integral. Using the two points $t = 0$ (where by definition, $\bar{f}_0(t) \equiv 1$) and the Callan-Treiman point $\Delta_{K\pi}$ as subtraction points leads to:

$$\bar{f}_0(t) = \exp \left[\frac{t}{\Delta_{K\pi}} (\ln C - G(t)) \right], \quad (3.1)$$

with

$$G(t) = \frac{\Delta_{K\pi}(\Delta_{K\pi} - t)}{\pi} \int_{t_{K\pi}}^{\infty} \frac{ds}{s} \frac{\phi_0(s)}{(s - \Delta_{K\pi})(s - t - i\epsilon)}. \quad (3.2)$$

Here, $\phi_0(s)$ is the phase of $\bar{f}_0(s)$. In writing Eq. (3.1), it has been assumed that $\bar{f}_0(t)$ has no zeros. We will come back to this point in Sec. 4.3. In what follows, $G(t)$ is decomposed as

$$G(t) = G_{K\pi}(\Lambda_S, t) + G_{as}(\Lambda_S, t) \pm \delta G(t), \quad (3.3)$$

where the first term corresponds to an integration from the threshold $t_{K\pi}$ up to a cut-off Λ_S which characterizes the end of the elastic region while in the second term the integration runs from Λ_S to ∞ . The choice of the value of Λ_S will be discussed later (see section 4.1). In the elastic or low-energy region ($t_{K\pi} < s < \Lambda_S$) the phase is identified with the s -wave, $I = 1/2$ $K\pi$ scattering phase, δ_0 , according to Watson's theorem [26]. In the analysis of Ref. [11], δ_0 (with its uncertainty) has been taken from Ref. [27]. There a matching of the solution of the Roy-Steiner equations with the $K\pi \rightarrow K\pi$, $\pi\pi \rightarrow K\bar{K}$ and $\pi\pi \rightarrow \pi\pi$ scattering data available at higher energies has been performed. The phase obtained in this way is in very good agreement with the work of Ref. [25], see below. In the inelastic or high-energy region ($s > \Lambda_S$), the phase is almost unknown. Perturbative QCD indicates [29] that $\bar{f}_0(t)$ vanishes as $\mathcal{O}(1/t)$ for large negative t . Thus from Eq. (3.2), we conclude that the phase must approach π asymptotically. In Ref. [11], the phase has been taken constant and equal to its asymptotic value of π for $s > \Lambda_S$ and an uncertainty of $\pm\pi$ has been assumed. Note that this uncertainty is a rather conservative estimate leading to a large band going from 0 to 2π . However, due to the two subtractions $G(t)$ converges rapidly, hence $G(t)$ is almost insensitive to the high energy behaviour of the phase, cf. Sec. 4.1, and the large uncertainty on the phase at high energy turns into a small uncertainty on $G(t)$. For example, $G(0)$, which has the largest error, is given for $\Lambda_S = 2.77 \text{ GeV}^2$ by

$$G(0) = 0.0398 \pm 0.0018 \pm 0.0036 \pm 0.0017, \quad (3.4)$$

where the first/second error correspond to the error on $G_{K\pi}/G_{a.s.}$, respectively, and the third error comes from the study of isospin breaking. We will come back to the uncertainties on $G(t)$ in detail in section 4.2.

The only free parameter, $\ln C$, in Eq. (3.1) could, in principle, be determined from the sum rule

$$\ln C = G(-\infty) \equiv \frac{\Delta_{K\pi}}{\pi} \int_{t_{\pi K}}^{\infty} \frac{ds}{s} \frac{\phi_0(s)}{(s - \Delta_{K\pi})}, \quad (3.5)$$

dictated by the asymptotic behaviour of $\bar{f}_0(t)$, cf. Ref. [29]. However, this sum rule, which exhibits one less subtraction than $G(t)$, Eq. (3.2), is not precise enough to allow to determine $\ln C$ with a good accuracy without adding any information on the high energy behaviour of the phase of the form factor. We will come back to the discussion of this sum rule later. Thus, $\ln C$ is a free parameter which can be determined from experiment by fitting the $K_{\mu 3}$ -decay distribution with the dispersive formula for $\bar{f}_0(t)$, Eq. (3.1). For more details on the dispersive representation of the scalar form factor, see Ref. [11].

3.2 Vector form factor

In connection with the recent precise measurements of the differential spectrum of the $\tau \rightarrow \nu_{\tau} K \pi$ decay by Belle [30] and BaBar [31], theoretical work has been devoted in the last few years to the description of $f_+(t)$. Form factors have been obtained in the framework of resonance chiral theory with additional constraints from dispersion relations in Refs. [32, 33]. In Ref. [34], a coupled channel analysis has been performed taking into account, through analyticity requirements, the experimental information on elastic and inelastic $K\pi$ scattering from the LASS collaboration. All these studies impose constraints from short distance QCD as well as the value of the vector form factor at zero momentum transfer. A fit to the τ data allows them to determine completely the shape of the form factor and thus to deduce a value for the slope and the curvature which compares reasonably well with the recent $K_{\ell 3}$ experiments. In these works, the emphasis is put on the energy region of the τ -decay and they are thus best suited for it. Here our aim is somewhat different: we want to have a very precise parametrization of the form factor at low energy improving on the pole parametrization usually assumed in the $K_{\ell 3}$ -analysis

$$\bar{f}_+(t) = \frac{M_V^2}{M_V^2 - t}, \quad (3.6)$$

which expresses the vector form factor completely in terms of a resonance described as a discrete pole at $\sqrt{t} = M_V$. This parametrization is physically motivated by the dominance of the $K^*(892)$ resonance in the vector channel. We will add to our knowledge of the presence of this resonance, the properties of analyticity and a proper behaviour of the phase at threshold. Contrary to the analysis discussed previously, we will not be able to determine the slope of the vector form factor but it will be a free parameter to be determined from a fit to the $K_{\ell 3}$ -data. This will allow us, using a twice subtracted dispersion relation as in the scalar case, to minimize the effect of the high energy region in the dispersive integral over the phase of the form factor.

In the case of the vector form factor, the value of $\bar{f}_+(t)$ at $t = 0$ is known, see Eq. (2.3), but there is no equivalence of the low-energy theorem of Callan and Treiman, Eq. (2.4). Thus

a dispersion relation for $\text{Ln}\bar{f}_+(t)$, this time twice-subtracted at zero, will be written. Defining $|d\bar{f}_+(t)/dt|_{t=0} \equiv \Lambda_+/m_\pi^2$ and assuming again that the form factor has no zero, this will be discussed in section 4.3, one has:

$$\bar{f}_+(t) = \exp\left[\frac{t}{m_\pi^2} (\Lambda_+ + H(t))\right], \text{ where } H(t) = \frac{m_\pi^2 t}{\pi} \int_{t_{K\pi}}^{\infty} \frac{ds}{s^2} \frac{\phi_1(s)}{(s-t-i\epsilon)}, \quad (3.7)$$

with $\phi_1(s)$ being the phase of $\bar{f}_+(s)$. At sufficiently low energies, in the elastic region, $\phi_1(s)$ is given by the p -wave, $I = 1/2$ $K\pi$ scattering phase, $\delta_{K\pi}^{I=1, I=1/2}(s) \equiv \delta_1(s)$. A detailed partial-wave analysis of $K\pi \rightarrow K\pi$ scattering in the energy range $s_0 \equiv (0.825 \text{ GeV})^2 \leq s \leq (2.5 \text{ GeV})^2$ has been performed in Ref. [27] based on high statistics production experiments. In order to reliably evaluate the dispersion integral, Eq. (3.7), an accurate extrapolation of the scattering phase down to threshold is needed. Contrary to the s -wave case, the Roy-Steiner equations are not really useful for providing such an extrapolation due to the lack of relevant experimental results. However, the well known method due to Gounaris and Sakurai [36] can be used to directly construct a partial wave amplitude which is unitary, has the correct threshold behaviour, the correct analyticity properties (neglecting the left-hand cut) and reproduces the position and width of the $K^*(892)$ as given by the PDG [21]. It is most suited to use the inverse amplitude method. Defining the function $D(s)$ via the T -matrix as

$$T = \frac{q_{K\pi}^2(s)}{D(s)}, \quad (3.8)$$

allows to determine its discontinuity

$$\text{Im } D(s) = -2 \frac{q_{K\pi}^3}{\sqrt{s}}. \quad (3.9)$$

Hence, one can write a dispersive representation for $1/T$ leading to

$$D(s) = -2q_{K\pi}^2(s) \frac{s}{\pi} \int_{t_{K\pi}}^{\infty} \frac{dx}{x} \frac{q_{K\pi}(x)}{\sqrt{x}} \frac{1}{x-s} + P(s) \quad (3.10)$$

with $P(s)$ being a subtraction polynomial. In the previous equations, we have used the standard notations,

$$s = (p_K + p_\pi)^2, \quad q_{K\pi}(s) = \frac{((s - (m_K + m_\pi)^2)(s - (m_K - m_\pi)^2))^{1/2}}{2\sqrt{s}}, \quad (3.11)$$

where $q_{K\pi}$ is the absolute value of the three-momentum in the $K\pi$ center of mass frame. Thus the $K\pi$ scattering phase is given by:

$$\frac{q_{K\pi}^3(s)}{\sqrt{s}} \text{ctg}(\delta_1(s)) = q_{K\pi}^2(s) h(s) + \frac{P(s)}{2}, \quad (3.12)$$

with

$$h(s) = -\frac{s}{\pi} \text{P} \int_{t_{K\pi}}^{\infty} \frac{dx}{x} \frac{q_{K\pi}(x)}{\sqrt{x}} \frac{1}{x-s}. \quad (3.13)$$

A minimal choice will be done here for $P(s)$ namely

$$P(s) = a + bs, \quad (3.14)$$

since it already gives a very good description of the phase in the vicinity of the resonance $K^*(892)$ and down to threshold. We will consider the impact of a higher order polynomial in section 4.2.2. The constants a and b are determined from the mass and the width of the $K^*(892)$ characterized as

$$\text{ctg}(\delta_1(s))|_{s=M_{K^*}^2} = 0 \quad \text{and} \quad \left. \frac{d\delta_1(s)}{ds} \right|_{s=M_{K^*}^2} = \frac{1}{M_{K^*}\Gamma_{K^*}}. \quad (3.15)$$

Note that there exists in the literature another definition of mass and width in terms of the position of the pole in the complex plane. The latter is process independent. The uncertainties coming from the inputs used for M_{K^*} and Γ_{K^*} will be discussed in section 4.2.2. Another possibility would be to determine a and b from a direct fit to the data [35]. This would, however, lead to a function $H(t)$ lying within the error bars discussed below. We checked that the phase constructed in this way with no free parameters leads to values of the p -wave scattering length, $a_1 = 0.0183m_\pi^2$, agreeing with other determinations [27, 37, 38].

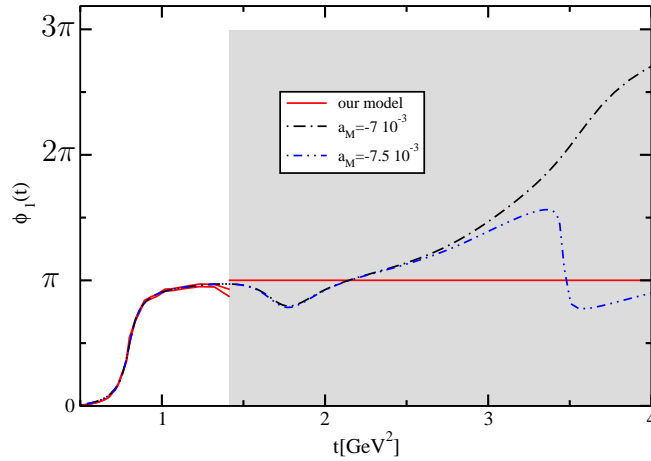


Figure 2: Comparison of our model for the phase of the vector form factor, Eq. (3.12), with the coupled channel analysis of Ref. [34]. The grey band corresponds to the assumption that above Λ_V the phase equals $\pi_{-\pi}^{+\pi}$, see text.

In p -wave scattering, inelasticity effects which imply $\phi_1(s) \neq \delta_1(s)$ become important at lower energies than in the scalar case, the mass of the vector resonance $K^*(1414)$ being an indication of the start of the inelasticity. At high energy, following the same arguments on the asymptotic behaviour as for the scalar case, the phase will reach its asymptotic value, π . Therefore, similarly to what has been done for $G(t)$, the function $H(t)$, Eq. (3.7), is decomposed into two parts:

$$H(t) = H_{K\pi}(\Lambda_V, t) + H_{as}(\Lambda_V, t) \pm \delta H(t), \quad (3.16)$$

with

$$H_{K\pi}(\Lambda_V, t) = \frac{m_\pi^2 t}{\pi} \int_{t_{K\pi}}^{s_0} \frac{\delta_1(t')}{t'^2(t'-t)} dt' + \frac{m_\pi^2 t}{\pi} \int_{s_0}^{\Lambda_V} \frac{\delta_{exp}(t')}{t'^2(t'-t)} dt', \quad (3.17)$$

and

$$H_{as}(\Lambda_V, t) = \frac{m_\pi^2 t}{\pi} \int_{\Lambda_V}^{\infty} \frac{\pi}{t'^2(t'-t)} dt' = -\frac{m_\pi^2}{t} \ln\left(1 - \frac{t}{\Lambda_V}\right) - \frac{m_\pi^2}{\Lambda_V}. \quad (3.18)$$

In these equations, Λ_V denotes the end of the elastic region. In what follows, we will use $\Lambda_V = (1.414)^2 \text{ GeV}^2$ and we will discuss other values for Λ_V in section 4.2.2. In Eq. (3.17),

the analytic formula for the phase δ_1 , Eq. (3.12), is used below s_0 . Above s_0 and below Λ_V the experimental points of Aston et al. [35] are used to determine δ_{exp} and to evaluate the corresponding contribution to $H(t)$ together with its uncertainties. As in the scalar case, the asymptotic contribution, Eq. (3.18), gives only a very small contribution to $H(t)$ due to the two subtractions. For the error, we will take a somewhat larger band than in the scalar case. Indeed it was found in Ref. [34] that a fit to the τ data reproducing the rate $R_{K\pi}$ quoted by the PDG [21] and compatible with asymptotic QCD, leads to a phase of the vector form factor reaching 3π at infinity. Thus we will take

$$\delta H_{as}(\Lambda_V, t) = \frac{+2H_{as}(\Lambda_V, t)}{-H_{as}(\Lambda_V, t)} \quad , \quad (3.19)$$

corresponding to the assumption that above Λ_V , $\phi_1(s) = \pi_{-\pi}^{+2\pi}$. This recipe almost certainly overestimates the real uncertainty. The other sources of uncertainty will be discussed in section 4.2.2. Let us give here only as an indication the value of H at t_0 , point in the physical region of $K_{\ell 3}$ -decay where it has the largest error. For $\Lambda_V = (1.414 \text{ GeV})^2$, one has

$$H(t_0) = (2.16 \pm 0.04_{-0.33}^{+0.65}) \times 10^{-3} \quad , \quad (3.20)$$

where the first uncertainty is the one on $H_{K\pi}$ and the second one the one on H_{as} , Eq. (3.16). Note that as for $G(t)$, even if the inelasticity sets in at lower energies, the uncertainty on the value of $H_{as}(\Lambda_V, t)$ related to our poor knowledge of $\phi_1(s)$ for $s > \Lambda_V$ is small due to the two subtractions performed this time at zero. The resulting phase, $\phi_1(t)$, with its uncertainties (grey band) is displayed in Fig. 2 using the charged K^* mass, $M_{K^*} = 891.66 \text{ MeV}$ and width $\Gamma_{K^*} = 50.8 \text{ MeV}$ from PDG [21]. It is compared with the phase obtained in Ref. [34] from two fits characterised by a different value of the parameter a_M , see Ref. [34] for more details.

Finally, let us note that a sum rule comparable to Eq. (3.5) is implied by the asymptotic behaviour of the form factor,

$$\Lambda_+ = -H(-\infty) = -\frac{m_\pi^2}{\pi} \int_{t_{K\pi}}^{\infty} ds \frac{\phi_1(s)}{s^2} \quad . \quad (3.21)$$

4 Discussion of errors and assumptions

The aim of the dispersive representation is to describe the shape of the form factor in the physical region of $K_{\ell 3}$ -decays as precisely as possible and consequently to test the Standard Model through the value of the scalar form factor at the Callan-Treiman point. In order to achieve this, it is mandatory to have under control all the assumptions entering the construction of the form factors as well as the determination of the errors. In the following, we will discuss the choice of the cut-off, the dependence on the input parameters and the absence of zeros.

4.1 Cut-off dependence

As just discussed two energy regions are distinguished in the dispersive analysis of the $K\pi$ form factors, the elastic one at low energy which is very well under control and the inelastic one at

higher energies which is of less importance in the description of the form factors due to the two subtractions in the dispersive representation. As explained before, in the latter region a rough estimate of the phase is made, using $\phi_0(t) = \pi \pm \pi$ for the scalar form factor and $\phi_1(t) = \pi_{-\pi}^{+2\pi}$ for the vector one. Let us first discuss this approximation in a bit more detail.

In Fig. 3, we show the phase of the scalar form factor as obtained from a once subtracted dispersion relation by Jamin et al., Ref. [25], as well as the phase of the $K\pi$ amplitude obtained by Büttiker et al., Ref. [27]. As can be seen, in the elastic region both phases agree as they

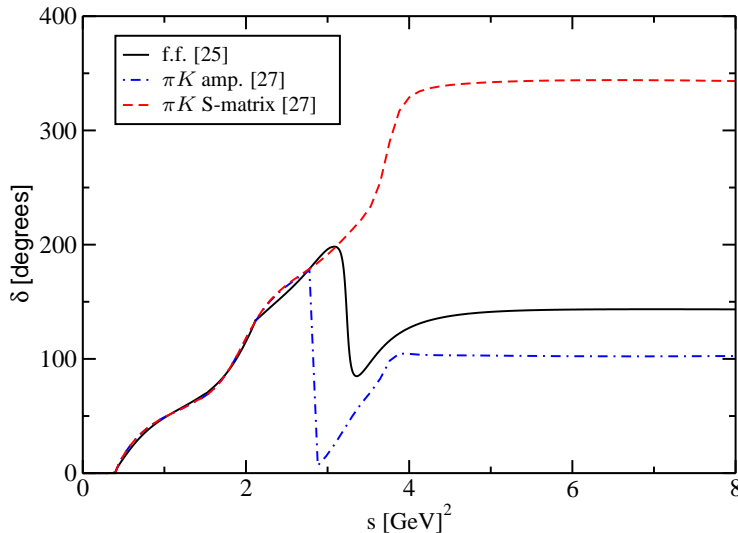


Figure 3: Comparison of the $K\pi$ scattering phases from the amplitude and the S -matrix in the scalar channel extracted in Ref. [27] and the phase of the form factor (preferred fit 6.10K2) obtained via a multi-channel analysis [25].

should. In the region where the inelasticity sets in both phases decrease, even rather abruptly in the case of the phase of the amplitude, and then start to grow again. This behaviour is well understood and has been explained in Refs. [39, 40] in the case of the scalar $\pi\pi$ form factor. Even though the central value of the phase discussed in section 3.1 does not have this property, the large uncertainty assigned to it takes it into account. Unless the form factor has a zero at some higher energy, as it will be discussed in the next section, no other sharp drop of the phase is expected and the phase will just in some way go to its asymptotic value π at very large t as typically does the phase obtained by Jamin et al. in Ref. [25]. Thus $\phi_0(t) = \pi \pm \pi$ certainly encompasses the physical phase of the scalar form factor.

Another source of uncertainty comes from the fact that the energies Λ_S and Λ_V where the inelasticity cannot be neglected any more are not very well known. For the s -wave, Λ_S was chosen in Ref. [11] as the energy where the phase of the amplitude is experimentally found to be different from the phase of the S -matrix, namely at $s = (1.66 \text{ GeV})^2$ as shown in Fig. 3. In the case of the vector form factor, the $K^*(1414)$ resonance can be seen as an indication of the end of the elastic region. We want to investigate here how sensitive $G(t)$ and $H(t)$ are to variations of the cutoffs Λ_S and Λ_V within reasonable bounds. We will concentrate on $G(t)$, an analogous study on $H(t)$ leads to similar conclusions. In Fig. 4, the bands represent the possible values of $G(0)$, Eq. (3.2), and of $G(-\infty)$, Eq. (3.5), as a function of the cut-off where $G(0)$ has the largest uncertainty in the whole physical region of $K_{\ell 3}$ -decays. For the s -wave a reasonable range of

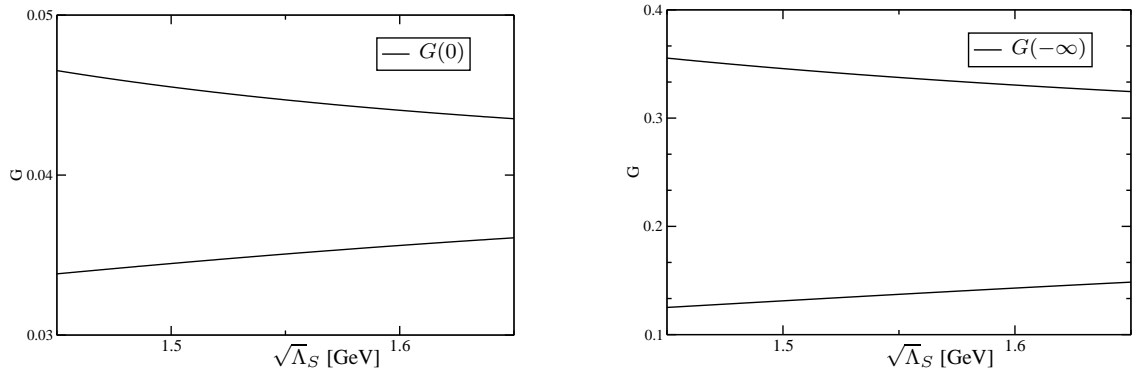


Figure 4: Variations of $G(0)$ (LHS) and $G(-\infty)$ (RHS) as a function of the end point of the elastic region Λ_S . Note that the scale differs in the two figures.

values for Λ_S is $(1.43 \text{ GeV})^2 < \Lambda_S < (1.66 \text{ GeV})^2$ where the lowest value is determined by the $K^*(1430)$ resonance. Within these limits $G_{min}(0)$ varies between 0.0331 and 0.0354 and $G_{max}(0)$ between 0.0474 and 0.0442 while $G_{min}(-\infty)$ varies between 0.1227 and 0.1495 and $G_{max}(-\infty)$ between 0.3599 and 0.3234 where $G_{max/min}(t) = G(t) \pm \delta G(t)$ and the plus sign corresponds to the maximum value. Hence although each part of the integral naturally depends on the exact cut-off value, the sum is clearly less sensitive on the exact position of Λ_S . We obtain, for instance, $G(0) = 0.0336 + 0.0067 = 0.0403$ for $\Lambda_S = (1.43 \text{ GeV})^2$ and $G(0) = 0.0362 + 0.0036 = 0.0398$ for $\Lambda_S = (1.66 \text{ GeV})^2$. As expected $G(-\infty)$, which involves one less subtraction, depends much more on the exact value of the cut-off and has a much larger uncertainty. However a comparison of the theoretical result for $\ln C$, Eq. (3.5), together with its experimental determinations [7, 3, 13], which lie between 0.14 to 0.21 show that the uncertainty on $G(t)$ is certainly overestimated. As already stated, a precise determination of $\ln C$ from the sum rule, Eq. (3.5), is in the actual state of the art not possible.

4.2 Variation of the input parameters

Within this section we will discuss the influence of the choice of the input parameters on the phase at low energies and therefore on the dispersive representation of the form factors.

4.2.1 Scalar form factor

At low energy the $I = 1/2$, s -wave $K\pi$ scattering phase, δ_0 from Ref. [27] is used in the evaluation of the function $G(t)$. As already discussed in Ref. [11], there are two sources of uncertainties on δ_0 . The first one comes from the propagation of the errors of the experimental inputs into the solution of the Roy-Steiner equations. The other one is due to the choice of the point where one matches the Roy-Steiner equations with the data. This leads to the conservative estimate (cf. Ref. [11]),

$$\delta G_{K\pi}(\Lambda_S, t) \leq 0.05 G_{K\pi}(\Lambda_S, t). \quad (4.1)$$

Furthermore, the analysis of Ref. [27] is performed under the assumption of perfect isospin

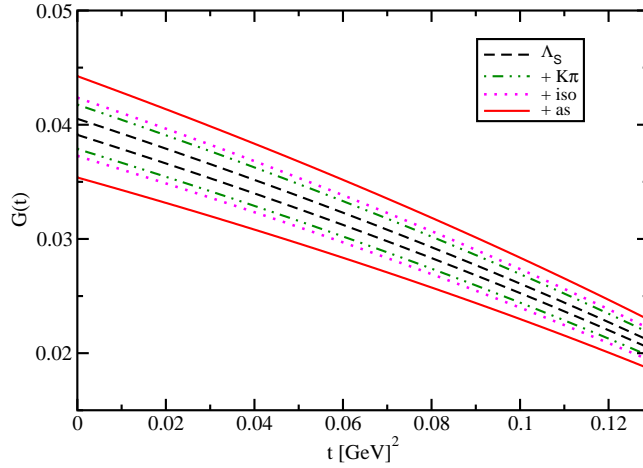


Figure 5: *The function $G(t)$ in the physical region. Each curve corresponds to one of the uncertainty discussed in the text added in quadrature to the previous one, in the order shown in the legend. The last curve gives the total uncertainty on $G(t)$.*

symmetry. In Ref. [41], it has been shown that for $\pi\pi$ scattering the shift in the phase due to isospin breaking corrections can amount up to 0.015. For the $\pi\pi$ system, these leading effects are of purely electromagnetic origin. In Refs. [42, 43] it has been argued that due to a partial cancellation between the strong and the electromagnetic effects, the total isospin breaking effect for $K\pi$ should be smaller than for $\pi\pi$. Awaiting a more detailed quantitative analysis [44], we will assume here as a conservative estimate of isospin breaking effects a constant shift of the phase by 0.02 which is even larger than the maximal value obtained for $\pi\pi$ [41]. The corresponding error on $G_{K\pi}(\Lambda_S, t)$ is, in fact, comparable to $\delta G_{K\pi}$, Eq. (4.1). Replacing the average values of m_K and m_π throughout the solution of Roy-Steiner equations with their physical ones has only a negligible effect on $G_{K\pi}(\Lambda_S, t)$.

The function $G(t)$ with the different uncertainties discussed here is plotted in Fig. 5. In section A.1 the simplified expression for $G(t)$ discussed in Ref. [11] is given together with the different errors on the parameters.

4.2.2 Vector form factor

To evaluate $H_{K\pi}$ we considered two domains as explained in section 3.2. From threshold $t_{K\pi}$ to s_0 the main input parameters are the mass and the width of the $K^*(892)$. Varying them within the error bars given by the PDG [21] has only a negligible influence on $H_{K\pi}$, the errors are at most a few 10^{-4} times $H_{K\pi}$. Another source of uncertainty in this energy region lies in the choice of the polynomial $P(s)$, Eq. (3.10). In order to estimate the effect of higher order terms, we added a contribution $c \cdot s^2$ to the r.h.s of Eq. (3.14) and varied the parameter c within $-0.15 \text{ GeV}^{-2} < c < 0.62 \text{ GeV}^{-2}$. Within this range we still obtain values for the scattering length, $a_1 m_\pi^3 = 0.013 - 0.020$, in agreement with other determinations [27, 37, 38] and the phases agree reasonably well with the Aston data as displayed in Fig. 6. The induced error on $H_{K\pi}$ is in this case a few 10^{-3} times its value. Between s_0 and the cutoff Λ_V the uncertainty on the phase is given by the error bars of the Aston data. To determine the error induced

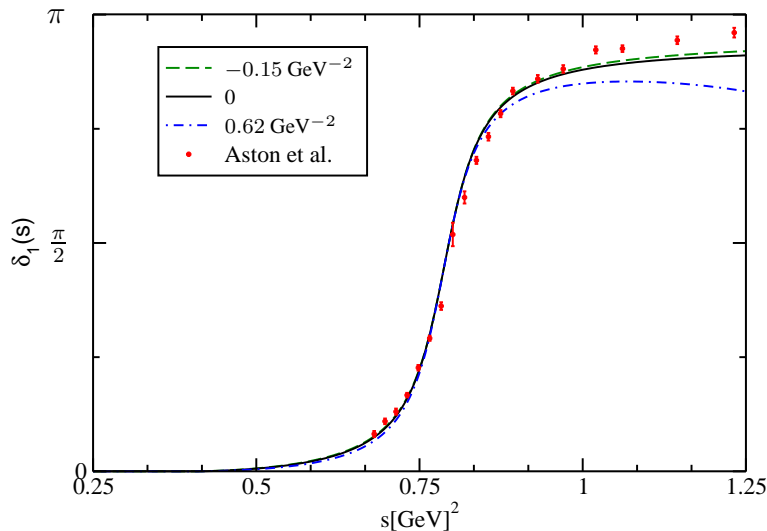


Figure 6: $K\pi$ scattering phase in the vector channel for different values of the parameter c . Here s_0 is fixed to the value $(0.825 \text{ GeV})^2$. For comparison the data [35] are shown, too.

by the choice of the cutoff values, we impose a rather large variation for s_0 and Λ_V , namely $(0.825 \text{ GeV})^2 < s_0 < (1.1 \text{ GeV})^2$ and $(1.2 \text{ GeV})^2 < \Lambda_V < (1.6 \text{ GeV})^2$.

The function $H(t)$ with the different uncertainties discussed here is plotted in Fig. 7. Except for H_{as} , we have symmetrized the errors which were not symmetric around the central value, using as error the largest value to be on the conservative side. In section A.2 a simplified expression for $H(t)$ is given together with the different sources of uncertainties on the parameters.

4.3 Discussion of possible zeros

Writing the dispersive relations, Eqs. (3.1, 3.7), we have assumed that the form factors have no zero. This is in fact quite standard when studying form factors. Indeed, in the space-like region, a form factor represents the Fourier transform of a charge density. It is argued for instance in Ref. [45] for the case of the electromagnetic form factor of the pion that the properties of the pion charge distribution should be similar to the one of the electron in the ground state of the hydrogen atom. This charge density being proportional to the square of the wave function, the corresponding form factor is positive in the space-like region. The possibility that the form factors have one or several zeros can, however, not be completely overruled and has been studied in the literature for example for the pion form factor in Ref. [46]. Let us therefore discuss it here for the scalar form factor. In the vector case the experimental situation is much better as we have seen in the introduction. Slope and curvature can be measured rather precisely. Zeros would essentially modify the relation between the slope and the curvature in the physical region of $K_{\ell 3}$ -decays compared to what we have been discussing here. Considering the precision of the experiment, allowed zeros cannot alter much the results in the physical region. We will however briefly mention what happens for the vector form factor in Sec. 4.3.4 in relation with the $\tau \rightarrow K\pi\nu_\tau$ decay.

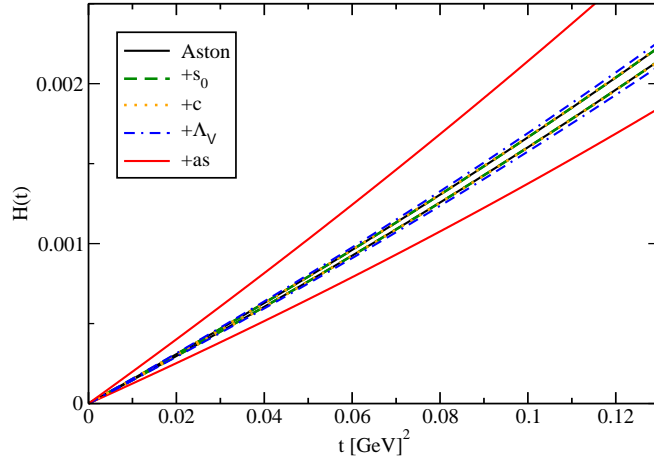


Figure 7: The function $H(t)$. Each curve corresponds to one of the uncertainty discussed in the text added in quadrature to the previous one, in the order shown in the legend. The last curve gives the total uncertainty on $H(t)$.

4.3.1 Real zeros

We will consider first one real zero, T_0 , to simplify. In that case the function $\bar{f}_0(t)/(1 - t/T_0)$ has no zero and one can proceed as in the previous section. One can thus write

$$\bar{f}_0(t) = \left(1 - \frac{t}{T_0}\right) \exp \left[\frac{t}{\Delta_{K\pi}} \left(\ln C - \ln \left(1 - \frac{\Delta_{K\pi}}{T_0}\right) - G(t) \right) \right]. \quad (4.2)$$

In order for $\bar{f}_0(t)$ to behave like $1/t$ for large negative t [29], the phase of the form factor has now to go to 2π at infinity since one has

$$\lim_{t \rightarrow -\infty} \bar{f}_0(t) = \text{const. } t/t^{\delta(+\infty)/\pi}. \quad (4.3)$$

Now there are two possibilities. The zero can be in the time-like or in the space-like region.

• **Time-like region** In the time-like region a zero on the real axis would correspond to a jump of the phase by π . In fact, Eq. (4.2) can be rewritten as

$$\bar{f}_0(t) = \exp \left[\frac{t}{\Delta_{K\pi}} \left(\ln C - \frac{\Delta_{K\pi}(\Delta_{K\pi} - t)}{\pi} \int_{t_{\pi K}}^{\infty} \frac{ds}{s} \frac{\phi_0(s) - \pi \theta(s - T_0)}{(s - \Delta_{K\pi})(s - t - i\epsilon)} \right) \right]. \quad (4.4)$$

Following the discussion of section 4.1, this zero should occur at a four momentum larger than $\sim (1.7 \text{ GeV})^2$ since below, the phase of $\bar{f}_0(t)$ is known and there is no indication of a zero for the form factor. At these energies there is a right-hand cut on the real axis and this scenario looks thus rather improbable. Furthermore since the region above Λ_S gives a small contribution to $G(t)$ in the $K_{\mu 3}$ -physical region, one does not expect much change in the form factor from the presence of such a zero. This is illustrated in Fig. 8 where a comparison is made between the form factor obtained from Eq. (3.1) and the one from Eq. (4.2) for $T_0 = 2.5 \text{ GeV}^2$. This is typically the smallest possible value for a real zero in this time-like region and thus the one which is expected to affect most our representation.

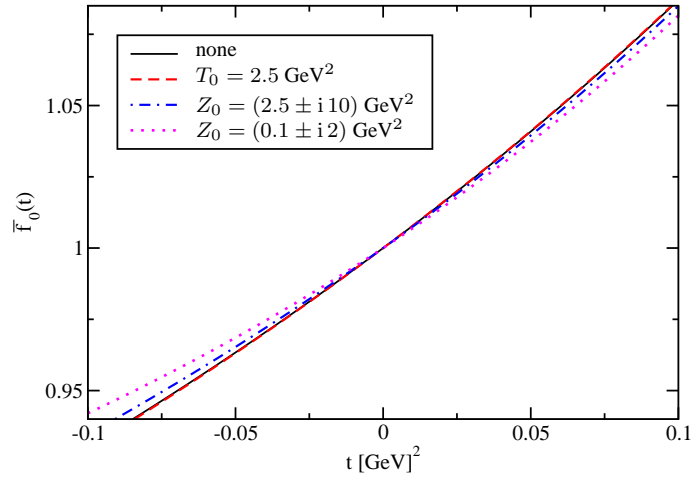


Figure 8: Scalar form factor: without zeros plain black curve, with a zero at $T_0 = 2.5 \text{ GeV}^2$, red dashed curve and with two complex conjugate zeros at $Z_0 = (2.5 \pm i 10) \text{ GeV}^2$, blue dashed-dotted curve and at $Z_0 = (0.1 \pm i 2) \text{ GeV}^2$ pink dotted curve.

• **Space-like region** In the space-like region, there is no left-hand cut and thus a real zero looks more plausible even though it goes against the argument of positivity of the form factor in the space-like region given previously. A completely different behaviour of the form factor as compared with the case without zero could result if the zero was close enough to the physical region. This can be seen in Fig. 9 where the scalar form factor is shown for two different values of T_0 , namely -0.1 GeV^2 and -1 GeV^2 . In the first case, the slope is rather large and there is a maximum at a rather small t value. As T_0 decreases, the slope becomes smaller and the maximum moves towards larger t and eventually approaches the curve without zero. This is in fact what happens for $T_0 = -1 \text{ GeV}^2$. The $K_{\mu 3}$ -data, however, seem to exclude the large slopes we observe when the zero becomes close to the physical region, see Fig. 9. In that case, the high energy behaviour of the form factor is completely different, too. This has an impact for instance in τ -decays as discussed below.

4.3.2 Complex zeros

Zeros could occur in the complex plane, which would in fact mean, due to the property of real-analyticity of the form-factor, the presence of a zero, Z_0 , and its complex conjugate \bar{Z}_0 . The form-factor would take the following form

$$\bar{f}_0(t) = \left(1 - \frac{t}{Z_0}\right) \left(1 - \frac{t}{\bar{Z}_0}\right) \exp \left[\frac{t}{\Delta_{K\pi}} \left(\ln C - \ln \left(1 - \frac{\Delta_{K\pi}}{Z_0}\right) - \ln \left(1 - \frac{\Delta_{K\pi}}{\bar{Z}_0}\right) - G(t) \right) \right]. \quad (4.5)$$

In order for $\bar{f}_0(t)$ to behave as $1/t$ for large negative t [29], the phase should now go asymptotically to 3π , see Eq. (4.3). As can be seen in Fig. 8, the presence of complex zeros could lead to lower values for the form factor at the end of the physical region. In the case of the blue dot-dashed curve which corresponds to zeros with rather large imaginary parts, namely $\pm 10 \text{ GeV}^2$ and a rather large real part, too, thus not close to the physical region of $K_{\mu 3}$ -decay, the difference to the curve without zero is very small as expected. The effect becomes, however,

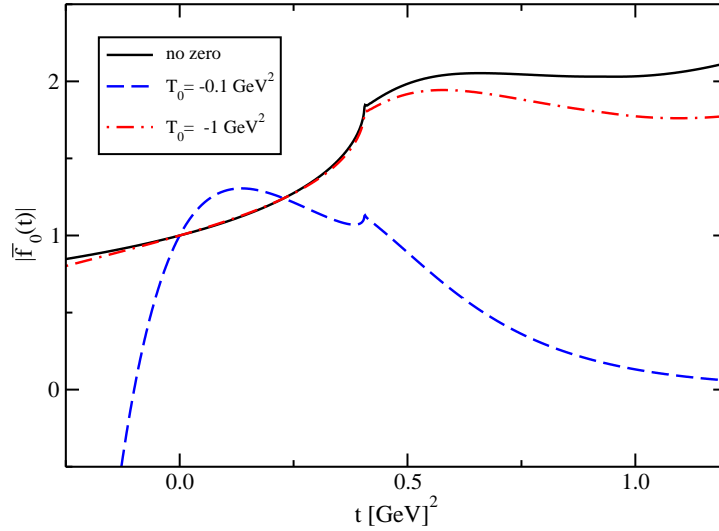


Figure 9: *Scalar form factor in presence of zeros located in the space-like region. Black plain curve: no zero, blue dashed/red dotted-dashed curves: real negative zero at $T_0 = -0.1 \text{ GeV}^2$ and -1 GeV^2 , respectively.*

much stronger when one takes a small real part as well as a smaller imaginary part, as shown by the pink dotted curve in Fig. 8 which corresponds to zeros at $(0.1 \pm i 2) \text{ GeV}^2$. The slope becomes smaller and the curvature larger. Note that the same value for $\ln C$ has been used in the determination of the curves, namely $\ln C = 0.2138$, Eq. (2.8) (the trends discussed here are independent of the precise value of $\ln C$) such that the three curves meet at the CT point.

4.3.3 Properties of the scalar form factor and their constraints on the existence of possible zeros

It is clear from the previous discussion that the presence of zeros in the scalar form factor with values close to the physical region would affect the determination of $\ln C$ from experiment. Unfortunately, it is not possible to test such a scenario with the $K_{\mu 3}$ -data since due to strong correlations and the sensitivity of the data it is only possible to determine one parameter for the scalar form factor from the fits. However, the scalar form factor possesses some properties which might allow to set up constraints on the presence or the absence of zeros. The different behaviour for t away from the physical region of $K_{\ell 3}$ -decays could have consequences, too, for example in τ -decays.

• **Sum rules** The first properties which can be used are sum rules which can be derived from the knowledge of the behaviour of the form factor for $t \rightarrow -\infty$. In the absence of zeros, one obtains the sum-rule, Eq. (3.5). It is modified in the presence of zeros and for instance, with one real zero, it reads

$$G(-\infty) = \ln C - \ln \left(1 - \frac{\Delta_{K\pi}}{T_0} \right). \quad (4.6)$$

The second logarithm on the right-hand side is negative so that the sum rule now leads to a value $G(-\infty)$ larger than $\ln C$. For example, with $T_0 = 2.5 \text{ GeV}^2$ as used above, one obtains

$\ln(1 - \Delta_{K\pi}/T_0) = -0.096$. Thus a good knowledge of these two quantities could provide an information on the presence of zeros in the form factor. In the case of complex zeros, one can derive two additional sum-rules namely

$$\int_{t_{K\pi}}^{\infty} ds \frac{\text{Im}\bar{f}_0(s)}{(1 - s/Z_0)(1 - s/\bar{Z}_0)} = 0, \quad (4.7)$$

$$\int_{t_{K\pi}}^{\infty} ds \frac{s \text{Im}\bar{f}_0(s)}{(1 - s/Z_0)(1 - s/\bar{Z}_0)} = 0. \quad (4.8)$$

All these sum rules have to be satisfied simultaneously. Unfortunately, they are rather sensitive to the phase at high energies which, as has already been stressed, is badly known. Consequently, they do not provide any constraint on the presence or absence of zeros as long as one does not have a better knowledge of the behaviour of this high energy phase. At present, it is possible to find a model for the phase which satisfies simultaneously the three sum rules.

• **Soft kaon analog of the Callan Treiman theorem** Another important property which provides us with a more severe constraint is the soft kaon analog of the Callan Treiman theorem [47]. One has

$$f_0(m_\pi^2 - m_K^2) = \frac{F_{\pi^+}}{F_{K^+}} + \tilde{\Delta}_{CT}. \quad (4.9)$$

A one loop calculation of the $SU(3)$ correction $\tilde{\Delta}_{CT}$ in the isospin limit [9] gives $\tilde{\Delta}_{CT} = 0.03$ which is larger than its soft pion analog Δ_{CT} , see Eq. (2.5), by a factor m_K^2/m_π^2 . It is rather small for a first order $SU(3) \otimes SU(3)$ breaking effect, which is expected to be of the order of 25%. Note one interesting point: at NLO within the minimal not-quite decoupling electroweak low-energy effective theory (LEET) [48], there appear in the light quark sector essentially two combinations of parameters of spurionic origin describing the couplings of quarks to the W -boson to be determined from experiment [49, 50]. While the knowledge of the scalar form factor at the CT point measures one combination, its knowledge at $m_\pi^2 - m_K^2$ measures the other one. A precise determination of $\tilde{\Delta}_{CT}$ would thus help to settle the issue of the presence of right-handed couplings of quarks to the W -boson. At present one can only give an estimate of the higher order contribution to $\tilde{\Delta}_{CT}$. The expected size is of the order of ten percent. To get an idea of the actual size, let us look at the two-loop calculation [51], where one finds:

$$\tilde{\Delta}_{CT} = 2 - \frac{F_K}{F_\pi} - \frac{F_\pi}{F_K} - \frac{16}{F_\pi^4} (2C_{12} + C_{34}) m_K^2 (m_K^2 - m_\pi^2) + \bar{\Delta}(m_\pi^2 - m_K^2) + \Delta(0). \quad (4.10)$$

The quantities $\bar{\Delta}(t)$ ⁷ and $\Delta(0)$ are discussed in Ref. [51], and C_{12} and C_{34} are two low energy constants (LECs). The same combination of these LECs in Eq. (4.10) appears in the two loop calculation of the slope, λ_0 , of the scalar form factor. Taking λ_0 between 0.009 and 0.016 which encompasses the values obtained by the NA48, KTeV and KLOE collaboration and using the value 1.22 for F_K/F_π as in Ref. [51] (for an actual status on the value of F_K/F_π , see for example Ref. [8]) one obtains $-4 \times 10^{-6} < 2C_{12} + C_{34} < 8 \times 10^{-6}$ in agreement with the estimates found in the literature [52, 53, 10, 18]. This leads to $-0.035 < \tilde{\Delta}_{CT} < 0.11$ within the expected order of magnitude. Assuming the Standard Model electroweak couplings, one

⁷Note that in Ref. [51] the parametrization of $\bar{\Delta}(t)$ is in principle only valid in the physical region. We will however use it here in order to get an estimate for $\tilde{\Delta}_{CT}$.

has $F_\pi/(F_K f_+(0)) = 0.8752 \pm 0.0020$, such that a conservative result for the normalized scalar form factor $\bar{f}_0(m_\pi^2 - m_K^2)$ is

$$0.8 < \bar{f}_0(m_\pi^2 - m_K^2) < 1. \quad (4.11)$$

This bound constrains the allowed region of possible zeros in the scalar form factor. Real zeros in the space-like region which do have an impact on the form factor in the physical region are excluded since they drop very fast with t for t negative and violate the bound. For complex zeros the situation is less obvious. It is easy to calculate which are the imaginary parts the complex zeros should have in order that the scalar form factor at $t = m_\pi^2 - m_K^2$ lies within the bound, Eq. (4.11). One finds that the positive imaginary part increases when the bound decreases. Typically for a complex zero with a real part between -0.2 and 0.2 the imaginary part varies between 0.7 for $\bar{f}_0(m_\pi^2 - m_K^2) = 1.03$ and 6 for $\bar{f}_0(m_\pi^2 - m_K^2) = 0.87$. Thus, with our present knowledge of $\tilde{\Delta}_{CT}$, one cannot totally eliminate the presence of complex zeros very close to the physical region which would affect the determination of $\ln C$.

4.3.4 High energy behaviour and the decay $\tau \rightarrow K\pi\nu_\tau$

The energy distribution in the decay $\tau \rightarrow K\pi\nu_\tau$ has been measured first by the ALEPH collaboration [54], then by OPAL [55], and recently the Belle collaboration [30] and the BaBar one [31] presented results for different isospin combinations. The cross section is described by

$$\frac{d\Gamma_{K\pi}(t)}{d\sqrt{t}} = \frac{V_{us}^2 G_F^2 m_\tau^3}{128\pi^3} q_{K\pi}(t) \left(1 - \frac{t}{m_\tau^2}\right)^2 \times \quad (4.12)$$

$$\left[\left(1 + \frac{2t}{m_\tau^2}\right) \frac{4q_{K\pi}^2(t)}{t} |f_+(t)|^2 + \frac{3(m_K^2 - m_\pi^2)^2}{t^2} |f_0(t)|^2 \right],$$

with the kinematic variable $q_{K\pi}$ defined in Eq. (3.11). It thus involves the scalar and the vector form factors. Unfortunately due to the presence of the $K^*(892)$ resonance which dominates the cross section between ~ 0.8 and ~ 1.2 GeV, one can only hope to obtain information on the scalar form factor from this decay channel very close to threshold. As discussed above, the only zeros which could lead to a clear difference in the energy distribution very close to the threshold are the real space-like zeros close to the $K_{\mu 3}$ -physical region. As is shown in Fig. 10 the curve is shifted towards larger values if there is no zero in the scalar form factor. The Belle data, seem to favor the latter even though the error bars are rather large for the lowest point⁸. This is consistent with the soft kaon analog of the CT theorem which, as we have seen, excludes the presence of such zeros in the scalar form factor.

On the right-hand side of the figure, the differential decay width, Eq. (4.12), is shown in a broader energy range and assuming the presence or absence of zeros in the vector form factor. The resonance region, where the contribution of the vector form factor dominates, becomes more sensitive to the phase in the inelastic region such that relatively large uncertainties for the decay width are expected in this resonance region. The dispersive representation without zero, for $\Lambda_+ = 0.02450$, and $\phi_1 = \pi$ beyond the cut off Λ_V , as discussed in section 3.2, describes amazingly well the precise Belle data in this region, see the central plain black curve on the

⁸ We do not show the BaBar data since they are not publicly available. The same trends hold, however, for them, too.

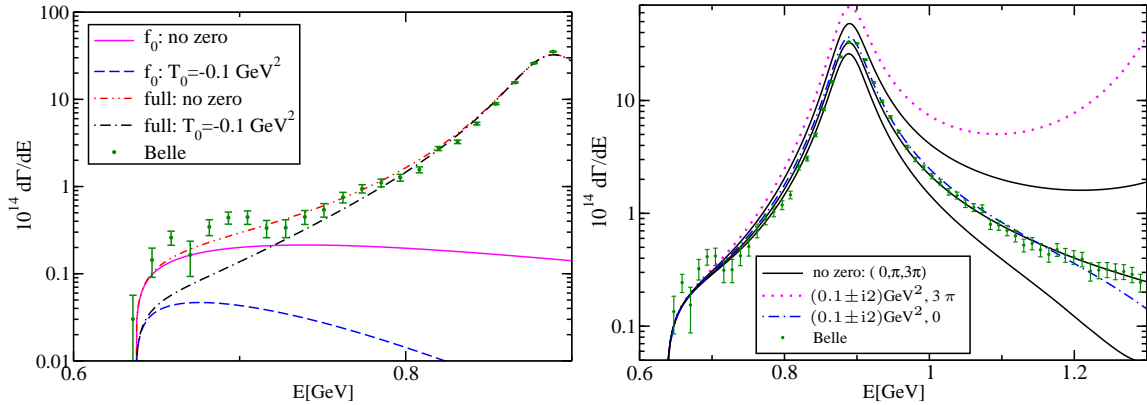


Figure 10: *Differential decay width $\tau \rightarrow K\pi\nu_\tau$. On the left-hand side the calculations with one real zero in the scalar form factor close to the physical region ($T_0 = -0.1 \text{ GeV}^2$) and without zero are compared. The vector form factor has no zero. On the right-hand side the calculation is done without zero and with complex zeros at $Z_0 = (0.1 \pm i2) \text{ GeV}^2$ in the vector form factor. Different cases have been considered corresponding to different ansätze for the phase as explained in the text. The scalar form factor has no zero. In these figures $\ln C = 0.2138$, Eq. (2.8) and $\Lambda_+ = 0.02450$ as obtained from the pole parametrization with the $K^*(892)$ mass. For comparison the Belle data for $\tau^- \rightarrow K_S^0\pi^-\nu_\tau$ [30] are displayed, too.*

RHS of Fig. 10. Much larger or smaller phases at the beginning of the inelastic region seem to be excluded as shown on the same figure where instead of π , 0 for the lower plain black curve and 3π for the upper plain black curve have been used for ϕ_1 . In the presence of complex zeros, on the contrary, the phase should be very small at the beginning of the inelastic region in order to reproduce the data, as illustrated in Fig. 10. There the result with a phase equal to 3π in the energy range from 1.4 to 3 GeV (pink dotted curve) is compared with the one with a vanishing phase in that same energy range (blue dashed curve). The opposite is true for real space-like zeros. As the value of T_0 increases, the resonance peak gets more and more washed out and eventually disappears for a given phase ϕ_1 . Rather highly improbable large values of the phase in the inelastic region becomes necessary to counterbalance the effect of the zeros. Thus from our study, due to the lack of knowledge of ϕ_1 in the inelastic (high-energy) region, we cannot completely rule out the presence of zeros in the vector form factor even though such a scenario does not seem very probable. We can, however, conclude as expected that zeros in the vector form factor which would not be totally excluded from the analysis of tau decays would not affect the low energy region of the vector form factor and consequently the results of the analysis of $K_{\ell 3}$ -decays.

5 Final remarks and Conclusion

In this paper we have discussed the robustness of a precise and convenient dispersive representation of the scalar and vector $K\pi$ form factors. In Fig.11 we show the scalar (left panel), Eq. (3.1), and the vector form factors (right panel), Eq. (3.7), with all the uncertainties discussed above under the usual assumption of no zeros in the form factors and for two different values of

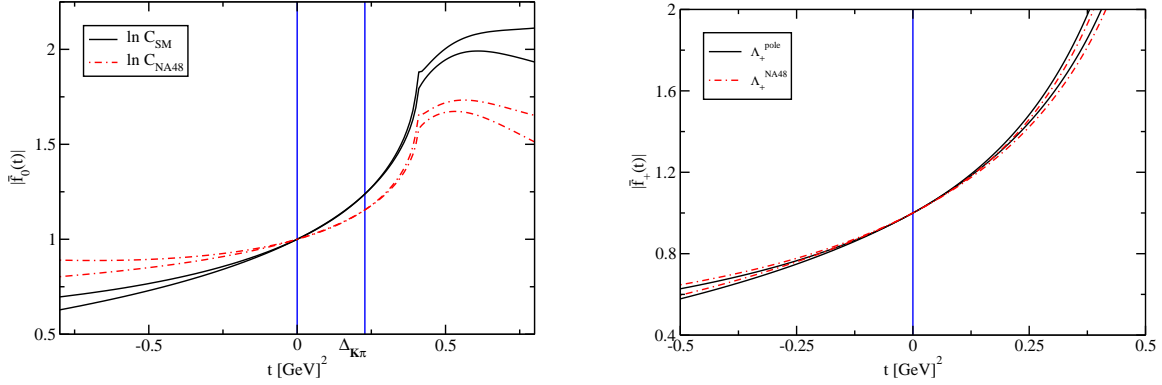


Figure 11: *Dispersive representation of the scalar (left panel) and vector (right panel) form factor over a wide range of energies. For comparison two different values of $\ln C$ (right) and Λ_+ (left) have been used: $\ln C|_{SM}$ is from Eq. (2.8), $\ln C|_{NA48} = 0.1438$, $\Lambda_+^{NA48} = 0.0233$ are the central values of the NA48 experimental results [7] and $\Lambda_+^{pole} = 0.02450$ is from the pole parametrization with the $K^*(892)$ mass. The band takes care of all the uncertainties discussed in the text.*

their respective free parameters $\ln C$ and Λ_+ . The figure nicely illustrates the fact that our dispersive representation describes to a very high accuracy the form factor shapes in the physical region of $K_{\ell 3}$ -decays. Eqs. (3.1, 3.7) thus represent a very useful tool for an optimal analysis of the $K_{\ell 3}$ -data. As already pointed out, it allows to determine the shape of these form factors in an unambiguous way, contrary to other parametrizations used in the data analysis. Furthermore, as emphasized in Ref. [11], a measurement of $\ln C$, with C the value of the normalized scalar form factor at the Callan-Treiman point, allows to test the Standard Model. A departure of the measured value from Eq. (2.8) would signal, under the hypothesis of no zeros in the form factor, a failure of the SM, as for example the presence of a direct coupling of right-handed quarks to W [11]. We have, however, to moderate slightly the conclusion drawn there. We have indeed seen that the shape of the scalar form factor could be slightly modified in the highly improbable case where it would have zeros in a very small domain of the complex plane within or close to the $K_{\mu 3}$ physical region. Even though the likelihood of this scenario is very small we have not been able at present to totally eliminate it. Note, however, that for the vector form factor, zeros that would affect the dispersive parametrization in the low energy region we are interested in here, are excluded by the tau data.

Acknowledgments:

We would like to thank H. Leutwyler for very useful and interesting discussions and a careful reading of the manuscript. We are grateful to B. Moussallam for enjoyable discussions and to him and M. Jamin for providing us with some of their results. One of us (E. P.) would like to thank I. Caprini and P. Minkowski for very interesting discussions. This work has been partially supported by the EU contract MRTN-CT-2006-035482 (“Flavianet”), by the European Community-Research Infrastructure Integrating Activity Study of Strongly Interacting Matter

(acronym HadronPhysics2, Grant Agreement n. 227431) under the Seventh Framework Programme of EU, by the Swiss National Science Foundation and by the IN2P3 theoretical project "Signature expérimentale des couplages électrofaibles non-standards des quarks".

A Some useful expressions

A.1 Scalar form factor

In order to facilitate and accelerate the numerical evaluation of the scalar form factor for example in the experimental analysis of $K_{\mu 3}^L$ -decays, it is convenient to have a parametrization of the function $G(t)$. As already discussed in Ref. [11], within the physical region it can be very accurately parametrized as

$$G_P(t) = xD + (1 - x)d + x(1 - x)k, \quad (\text{A.1})$$

where $x \equiv t/t_0$, $d \equiv G(0)$, $D \equiv G(t_0)$. The value of k can be obtained from the constraint $G(\Delta_{K\pi}) = 0$. In Table 1 we give the central values for the parameter d , D , k together with the corresponding errors arising from the different sources of errors as discussed in the previous section.

	Central value	δG_Λ	δG_{as}	$\delta G_{K\pi}$	$\delta G_{isospin}$	total error
d	0.0398	0.0005	0.0036	0.0018	0.0017	0.0044
D	0.0209	0.0002	0.0016	0.0010	0.0010	0.0021
k	0.0045	0.0000	0.0001	0.0002	0.0003	0.0004

Table 1: Coefficients arising in the parametrization G_P with their uncertainties.

For practical purposes and for comparison with the traditionally often used linear and quadratic approximations to the form factor, it is useful to list the first coefficients of the Taylor expansion of the form factor. They read

$$\begin{aligned} \frac{1}{m_\pi^2} \left. \frac{d\bar{f}_0}{dt} \right|_{t=0} &= \frac{m_\pi^2}{\Delta_{K\pi}} (\ln C - G(0)) = \frac{m_\pi^2}{\Delta_{K\pi}} (\ln C - 0.0398(44)), \\ \frac{1}{m_\pi^4} \left. \frac{d^2\bar{f}_0}{dt^2} \right|_{t=0} &= \left(m_\pi^2 \left. \frac{d\bar{f}_0}{dt} \right|_{t=0} \right)^2 - 2 \frac{m_\pi^4}{\Delta_{K\pi}} G'(0) = \left(m_\pi^2 \left. \frac{d\bar{f}_0}{dt} \right|_{t=0} \right)^2 + (4.16 \pm 0.56) \times 10^{-4}, \\ \frac{1}{m_\pi^6} \left. \frac{d^3\bar{f}_0}{dt^3} \right|_{t=0} &= \left(m_\pi^2 \left. \frac{d\bar{f}_0}{dt} \right|_{t=0} \right)^3 - 6 \frac{m_\pi^4}{\Delta_{K\pi}} G'(0) \left(m_\pi^2 \left. \frac{d\bar{f}_0}{dt} \right|_{t=0} \right) - 3 \frac{m_\pi^6}{\Delta_{K\pi}} G''(0) \\ &= \left(m_\pi^2 \left. \frac{d\bar{f}_0}{dt} \right|_{t=0} \right)^3 + 3 (4.16 \pm 0.56) \times 10^{-4} \left(m_\pi^2 \left. \frac{d\bar{f}_0}{dt} \right|_{t=0} \right) + (2.72 \pm 0.21) \times 10^{-5}. \end{aligned} \quad (\text{A.2})$$

The Taylor expansion up to third order of the scalar form factor allows to well reproduce the exact dispersive representation in the physical region. The maximal error is 3%.

A.2 Vector form factor

It is equally very convenient to have a parametrisation of the function $H(t)$ in order to avoid the evaluation of the dispersive integral for the vector form factor. Within the physical region, the function $H(t)$ can be very accurately parametrized as

$$H_P(t) = H_1 x + H_2 x^2 . \quad (\text{A.3})$$

The numerical values of the parameters H_1 and H_2 are given in Table 2 together with the corresponding uncertainties. As discussed in the text, the uncertainties coming from the uncertainties on the mass and the width of the K^* , $\delta H_{M_{K^*}}$ and $\delta H_{\Gamma_{K^*}}$ are completely negligible. Here again,

	Central value	δH_{Aston}	δH_{s_0}	δH_c	δH_{Λ_V}	δH_{as}	total error
$H_1 \times 10^3$	1.92	0.04	0.01	0.01	0.06	+0.62 -0.31	+0.63 -0.32
$H_2 \times 10^4$	2.63	0.04	0.01	0.02	0.04	+0.27 -0.13	+0.28 -0.15

Table 2: Coefficients arising in the parametrization H_P with their different uncertainties.

for practical purposes and for comparison with other parametrizations of the vector form factor, it is useful to give the first coefficients of the Taylor expansion

$$\begin{aligned} m_\pi^2 \left. \frac{d\bar{f}_+}{dt} \right|_{t=0} &= \Lambda_+ , \\ m_\pi^4 \left. \frac{d^2\bar{f}_+}{dt^2} \right|_{t=0} &= \Lambda_+^2 + 2m_\pi^2 H'(0) = \Lambda_+^2 + (5.79_{-0.97}^{+1.91}) \times 10^{-4} , \\ m_\pi^6 \left. \frac{d^3\bar{f}_+}{dt^3} \right|_{t=0} &= \Lambda_+^3 + 6m_\pi^2 H'(0)\Lambda_+ + 3m_\pi^4 H''(0) = \Lambda_+^3 + 3(5.79_{-0.97}^{+1.91}) \times 10^{-4} \Lambda_+ \\ &\quad + (2.99_{-0.21}^{+0.39}) \times 10^{-5} . \end{aligned} \quad (\text{A.4})$$

The third order Taylor expansion is very accurate in this case, too. The maximal error with respect to the exact dispersive representation is 6%.

A.3 Calculation of I_K

In order to extract $|f_+(0)V_{us}|$ from the measurement of the $K_{\ell 3}$ decay rate

$$\Gamma_{K_{\ell 3}^{+/\ 0}} = \mathcal{N}_{K^{+/\ 0}} S_{EW} (1+2\Delta_{K^{+/\ 0}\ell}^{EM}) |f_+^{K^{+/\ 0}}(0)V_{us}|^2 I_{K^{+/\ 0}}^\ell , \quad \mathcal{N}_{K^{+/\ 0}} = C_{K^{+/\ 0}}^2 G_F^2 m_{K^{+/\ 0}}^5 / (192\pi^3) , \quad (\text{A.5})$$

one has to evaluate the phase space integrals $I_{K^{+/\ 0}}^\ell$ defined in terms of the scalar and vector form factors:

$$I_{K^{+/\ 0}}^\ell = \int_{m_\ell^2}^{t_0} dt \frac{1}{m_{K^{+/\ 0}}^8} \lambda^{3/2} \left(1 + \frac{m_\ell^2}{2t} \right) \left(1 - \frac{m_\ell^2}{2t} \right)^2 \left(\bar{f}_+^2(t) + \frac{3m_\ell^2 \Delta_{K\pi}^2}{(2t + m_\ell^2)\lambda} \bar{f}_0^2(t) \right) . \quad (\text{A.6})$$

Using the dispersive parametrization for the form factors, see Eqs. (3.1, 3.7), it is possible for practical purpose, to approximate the phase space integrals, Eq. (A.6), by a polynomial expansion in terms of the two parameters $\ln C$ and Λ_+ entering this parametrization. One obtains

$$I_{K^{+/\ell}}^\ell = c_0 + c_1\Lambda_+ + c_2\Lambda_+^2 + c_3\Lambda_+^3 + c_4\Lambda_+^4 + c_5\ln C + c_6\ln C^2 + c_7\ln C^3 + c_8\ln C^4, \quad (\text{A.7})$$

where the polynomial coefficients for the 4 phase-space integrals are collected in the following table:

	c_0	c_1	c_2	c_3	c_4	c_5	c_6	c_7	c_8
$I_{K^0}^e$	0.14126	0.48960	1.35655	3.12372	6.14597	–	–	–	–
$I_{K^0}^\mu$	0.09061	0.29599	0.95764	2.36194	4.81855	0.01724	0.00515	0.00120	0.00023
$I_{K^+}^e$	0.14530	0.53899	1.59964	3.94735	8.32532	–	–	–	–
$I_{K^+}^\mu$	0.09324	0.32606	1.13005	2.98682	6.53170	0.01798	0.00545	0.00129	0.00025

Table 3: Coefficients of Λ_+ and $\ln C$, Eq. (A.7) in the polynomial expansion of the phase space integrals, Eq. (A.6).

References

- [1] O. P. Yushchenko *et al.*, Phys. Lett. B **581** (2004) 31 [arXiv:hep-ex/0312004]; O. P. Yushchenko *et al.*, Phys. Lett. B **589** (2004) 111 [arXiv:hep-ex/0404030].
- [2] F. Ambrosino *et al.* [KLOE Collaboration], Phys. Lett. B **636** (2006) 166 [arXiv:hep-ex/0601038].
- [3] F. Ambrosino *et al.* [KLOE Collaboration], JHEP **0712** (2007) 105 [arXiv:0710.4470 [hep-ex]].
- [4] T. Alexopoulos *et al.* [KTeV Collaboration], Phys. Rev. D **70** (2004) 092007 [arXiv:hep-ex/0406003].
- [5] E. Abouzaid *et al.* [KTeV Collaboration], Phys. Rev. D **74**, 097101 (2006) [arXiv:hep-ex/0608058].
- [6] A. Lai *et al.* A. Lai *et al.* [NA48 Collaboration], Phys. Lett. B **604** (2004) 1 [arXiv:hep-ex/0410065].
- [7] A. Lai *et al.* [NA48 Collaboration], Phys. Lett. B **647** (2007) 341 [arXiv:hep-ex/0703002].
- [8] M. Antonelli *et al.* [FlaviaNet Working Group on Kaon Decays], arXiv:0801.1817 [hep-ph].
- [9] J. Gasser and H. Leutwyler, Nucl. Phys. B **250** (1985) 517.
- [10] A. Kastner and H. Neufeld, Eur. Phys. J. C **57** (2008) 541 [arXiv:0805.2222 [hep-ph]].
- [11] V. Bernard, M. Oertel, E. Passemar and J. Stern, Phys. Lett. B **638** (2006) 480 [arXiv:hep-ph/0603202].

- [12] R. J. Hill, Phys. Rev. D **74**, 096006 (2006) [arXiv:hep-ph/0607108].
- [13] V. Bernard, M. Oertel, E. Passemar, J. Stern and the KTeV collaboration, in preparation.
- [14] C. G. Callan and S. B. Treiman, Phys. Rev. Lett. **16** (1966) 153; R. F. Dashen and M. Weinstein, Phys. Rev. Lett. **22** (1969) 1337.
- [15] J. Gasser and H. Leutwyler, Nucl. Phys. B **250** (1985) 517.
- [16] H. Leutwyler, private communication.
- [17] J. Bijnens and K. Ghorbani, arXiv:0711.0148 [hep-ph].
- [18] V. Bernard and E. Passemar, Phys. Lett. B **661** (2008) 95 [arXiv:0711.3450 [hep-ph]].
- [19] L. Lellouch, "Kaon Physics: A Lattice Perspective", Talk given at the XXVI International Symposium on Lattice Field Theory, July 14-19 2008, JLab, Virginia, USA, arXiv:0902.4545 [hep-lat].
- [20] E. Blucher and W. Marciano in Ref. [21].
- [21] C. Amsler *et al.* [Particle Data Group], Physics Letters **B667** (2008) 1.
- [22] J. C. Hardy and I. S. Towner, arXiv:0812.1202 [nucl-ex].
- [23] R. Omnès, Nuovo Cim. **8** (1958) 316; N. I. Muskhelishvili, Singular Integral Equations, Noordhoff Series of Monographs on Pure and Applied Mathematics, Groningen (1953).
- [24] J. F. Donoghue, J. Gasser and H. Leutwyler, Nucl. Phys. B **343** (1990) 341.
- [25] M. Jamin, J. A. Oller and A. Pich, Nucl. Phys. B **587** (2000) 279 [hep-ph/0006045]; *ibid*, Nucl. Phys. B **622** (2002) 279 [hep-ph/0110193].
- [26] K. M. Watson, Phys. Rev. **88** (1952) 1163.
- [27] P. Büttiker, S. Descotes-Genon and B. Moussallam, Eur. Phys. J. C **33** (2004) 409 [arXiv:hep-ph/0310283].
- [28] P. Estabrooks, R. K. Carnegie, A. D. Martin, W. M. Dunwoodie, T. A. Lasinski and D. W. G. Leith, Nucl. Phys. B **133** (1978) 490.
- [29] G. P. Lepage and S. J. Brodsky, Phys. Lett. B **87** (1979) 359.
- [30] D. Epifanov *et al.* [Belle Collaboration], Phys. Lett. B **654** (2007) 65 [arXiv:0706.2231 [hep-ex]].
- [31] B. Aubert *et al.* [BABAR Collaboration], Phys. Rev. D **76** (2007) 051104 [arXiv:0707.2922 [hep-ex]]; B. Aubert *et al.*, talk presented at ICHEP08, Philadelphia, Pennsylvania, [arXiv:0808.1121 [hep-ex]].
- [32] M. Jamin, A. Pich and J. Portoles, Phys. Lett. B **640** (2006) 176 [arXiv:hep-ph/0605096]; *ibid*, Phys. Lett. B **664** (2008) 78 [arXiv:0803.1786 [hep-ph]].

- [33] D. R. Boito, R. Escribano and M. Jamin, *Eur. Phys. J. C* **59** (2009) 821 [arXiv:0807.4883 [hep-ph]].
- [34] B. Moussallam, *Eur. Phys. J. C* **53** (2008) 401 [arXiv:0710.0548 [hep-ph]].
- [35] D. Aston *et al.*, *Nucl. Phys. B* **296** (1988) 493.
- [36] G. J. Gounaris and J. J. Sakurai, *Phys. Rev. Lett.* **21** (1968) 244.
- [37] V. Bernard, N. Kaiser and U.-G. Meißner, *Nucl. Phys. B* **357** (1991) 129.
- [38] A. Roessl, *Nucl. Phys. B* **555** (1999) 507 [arXiv:hep-ph/9904230].
- [39] B. Ananthanarayan, I. Caprini, G. Colangelo, J. Gasser and H. Leutwyler, *Phys. Lett. B* **602** (2004) 218 [arXiv:hep-ph/0409222].
- [40] J. A. Oller and L. Roca, *Phys. Lett. B* **651** (2007) 139 [arXiv:0704.0039 [hep-ph]].
- [41] J. Gasser, *PoS KAON* (2008) 033 [arXiv:0710.3048 [hep-ph]]; G. Colangelo, J. Gasser and A. Rusetsky, *Eur. Phys. J. C* **2009** (2009) 1 [arXiv:0811.0775 [hep-ph]].
- [42] B. Kubis and U.-G. Meißner, *Nucl. Phys. A* **699** (2002) 709 [arXiv:hep-ph/0107199].
- [43] A. Nehme and P. Talavera, *Phys. Rev. D* **65** (2002) 054023 [arXiv:hep-ph/0107299].
- [44] V. Bernard, M. Knecht, M. Oertel, E. Passemar, work in progress.
- [45] H. Leutwyler, in *Continuous Advances in QCD 2002*, eds. K A. Olive, M. A. Shifman and M. B. Voloshin, World Scientific, Singapore (2003), p. 23, [hep-ph/0212324].
- [46] I. Raszillier, W. Schmidt and I.-Sabba Stefanescu, *Z. Phys. A* **277** (1976) 211.
- [47] R. Oehme, *Phys. Rev. Lett.* **16** (1966) 215.
- [48] J. Hirn and J. Stern, *Eur. Phys. J. C* **34** (2004) 447 [hep-ph/0401032]; *ibid*, *JHEP* **0409** (2004) 058 [hep-ph/0403017]; *ibid*, *Phys.Rev. D* **73** (2006) 056001 [arXiv:hep-ph/0504277].
- [49] J. Stern, *Nucl. Phys. Proc. Suppl.* **174** (2007) 109 [arXiv:hep-ph/0611127].
- [50] V. Bernard, M. Oertel, E. Passemar and J. Stern, *JHEP* **0801** (2008) 015 [arXiv:0707.4194 [hep-ph]].
- [51] J. Bijnens and P. Talavera, *Nucl. Phys. B* **669** (2003) 341 [arXiv:hep-ph/0303103].
- [52] M. Jamin, J. A. Oller and A. Pich, *JHEP* **0402** (2004) 047 [arXiv:hep-ph/0401080].
- [53] V. Cirigliano, G. Ecker, M. Eidemuller, R. Kaiser, A. Pich and J. Portoles, *JHEP* **0504** (2005) 006 [arXiv:hep-ph/0503108].
- [54] R. Barate *et al.* [ALEPH Collaboration], *Eur. Phys. J. C* **11** (1999) 599 [arXiv:hep-ex/9903015].
- [55] G. Abbiendi *et al.* [OPAL Collaboration], *Eur. Phys. J. C* **35** (2004) 437 [arXiv:hep-ex/0406007].